

BEAM COUPLING IMPEDANCES OF FERRITE-LOADED CAVITIES: CALCULATIONS AND MEASUREMENTS*

S. S. Kurennoy[†], R.C. McCrady, Los Alamos National Laboratory, Los Alamos, NM, USA

Abstract

We have developed an efficient method of calculating impedances in cavities with dispersive ferrite dampers. The ferrite dispersive properties in the frequency range of interest are fitted in CST, which allows using both wake field and lossy eigenmode solvers. A simple test cavity with or without ferrite inserts is explored both numerically and experimentally. The resonance frequencies and beam coupling impedances at cavity resonances are calculated with CST to understand the mode structure. The cavity transverse coupling impedances are also measured on a test stand using a two-wire method. We compare results of impedance calculations and measurements for a few different configurations, with and without ferrites, to ensure a complete understanding of the cavity resonances and their damping with ferrite. These results are important to provide an adequate damping of undesired transverse modes in induction-linac cells.

INTRODUCTION

Beam breakup (BBU) instability in high-current linear induction accelerators (LIA) limits the acceptable values of the transverse dipole beam coupling impedance, Z_{tr} ; see [1] and references therein. Reducing Z_{tr} is an important goal in designing LIA accelerating modules. This is often achieved by using ferrite absorbers that damp cavity modes in the frequency range important for beam stability; e.g. in the DARHT linacs [1]. The two-wire method for measuring transverse impedances has been established [2] but it requires having a fabricated LIA cell or its prototype for performing measurements. A reliable method of impedance calculation is needed to quickly evaluate and select design options, and thus guide the design process.

The main difficulty of impedance calculation for ferrite-loaded cavities is to properly account for dispersive properties of ferrites. The ferrite complex permeability $\mu = \mu' - j\mu''$ depends on frequency f . It means that in time domain the magnetic flux density $B(t)$ is defined not by an instantaneous value of field $H(t)$ but by its time convolution with Fourier transform $\mu(\tau)$ of $\mu(f)$. The code AMOS [3] can include dispersive ferrites and was historically used for modeling LIA cavities, but it is limited to axisymmetric structures. The more modern CST codes [4] also can be used for computations with dispersive materials. The data for ferrite properties are fitted in CST in a way that allows efficient Fourier transforms for computations. Using CST, we develop a method for calculating impedances of cavities with dispersive ferrites and compare its predictions with measurements for a simple test cavity.

* Work supported by NNSA, US Department of Energy.

[†] kurennoy@lanl.gov

TEST CAVITY

The test cavity is a short pancake-like cylindrical cavity on a beam pipe, all made of aluminum. The cavity length is 2.94" and its inner radius 13.37" = 34 cm. The beam pipe of inner radius 7.41 cm has length 19.08" = 48.5 cm, equal to the length of a prototype LIA [5] accelerating cavity. Both pipe ends have brass wave launchers (6" and 10" long) that support two parallel brass wires of 1/8" diameter spaced 4" apart inside the pipe. CST models of two setups are shown in Fig. 1; the vacuum part is transparent blue, walls are hidden. The cavity size was chosen to have two transverse dipole modes in the frequency range of interest, 100 MHz – 1 GHz, in the empty cavity. We had two ferrite sets for tests; both were spares from DARHT. They are shown in black in Fig. 1. One consists of two arcs of 146° with inner radius 20.2 cm and trapezoidal cross section of 1" height, shown in Fig. 1 (left) inset. The other ferrite is a toroid with inner radius 12.2 cm and cross section 1" x 3", Fig. 1 (right). The ferrites are supported by 1"-thick dielectric foam, General Plastics 3703 ($\epsilon = 1.06$), yellow in Fig. 1, with cutouts for ferrite pieces. The wires are shown in Fig. 1 in brown (right) or gray (left); the blue lines are the pipe axis and two parallel axes displaced by 1 cm in x or y . Details of the measurement setup are described in [1].

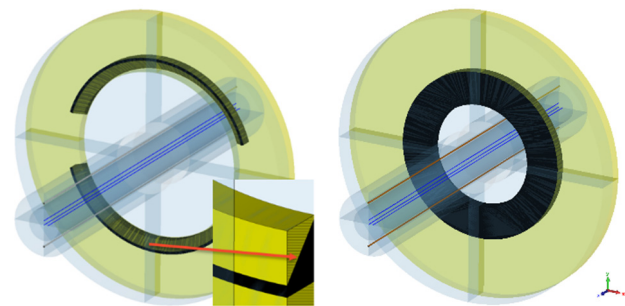


Figure 1: Two CST models of test cavity with ferrites.

FERRITE MATERIAL PROPERTIES

Our initial simulations were complicated by the fact that the exact type of the arc ferrite was unknown. The ring ferrite was likely PE11 from TDK; its permeability was measured and fitted in [6]. Since then we obtained data and also measured samples of other ferrites. Magnetic properties of some absorber ferrites are compared in Fig. 2, where fit [6] is marked DF. The ferrite losses are defined by μ'' ; ferrites PE11 and CN20 [7] provide higher losses. Note that measured permeability of PE11 is higher than in [6] and close to the measured one for ferrite 4F5 (not shown in Fig. 2) in this frequency range. The electric permittivity for all these ferrites does not change much in this range; typically, ϵ' is 10-12, and ϵ'' is small, <1 .

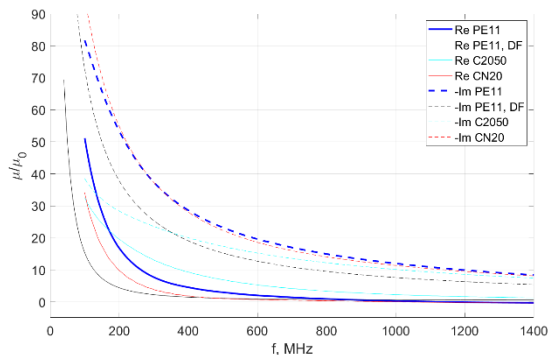


Figure 2: Real (solid curves) and imaginary (dashed) parts of magnetic permeability for a few absorbing ferrites.

IMPEDANCE CALCULATIONS

The transverse dipole modes of the empty cavity are calculated with CST eigensolver. The results are in Table 1, where Z_{tr} is the dipole transverse coupling impedance, Q -factor is for Al walls with conductivity $\sigma = 3.7 \cdot 10^7$ Sm/m. The frequencies measured with RF probes are very close. Including wires in simulations splits each mode in two.

Table 1: Transverse Dipole Modes of Empty Test Cavity

Mode	f , MHz	Q	Z_{tr} , Ω/m
E ₁₁₀	521.7	16,700	$2.45 \cdot 10^6$
E ₁₂₀	952.7	21,814	$2.64 \cdot 10^6$

Note that CST post-processing calculates the “structure” shunt impedance defined as $Z_{sh} = V^2/P_{av}$, where V is the voltage amplitude and P_{av} is the average dissipated power. The beam coupling impedance is defined as $Z_c = V^2/(2P_{av})$, see in [8]. The impedance values in Table 1 and below already include this extra factor $1/2$.

For ferrite-loaded test cavity, lossy eigenmodes are calculated with CST non-linear eigensolver. It solves for complex frequencies of modes with $Q > 1$. The imaginary part of frequency is related to its Q -factor. The results for the ring ferrite of Fig. 1 (right) are in Table 2. The second resonance is completely damped in this case.

Table 2: Transverse Dipole Modes With Ring Ferrite

Mode	f , MHz	Q	Z_{tr} , Ω/m
E ₁₁₀	476.2	5.28	1293
E ₁₂₀	-	-	-

The cavity with two arc ferrites, Fig. 1 (left), is asymmetric. The transverse impedance depends on the direction of beam offset from the axis: vertical (in y) and horizontal (in x) impedances are different; see results in Table 3.

Table 3: Transverse Dipole Modes With Two Arc Ferrites

Mode	f , MHz	Q	Z_{tr} , Ω/m
E _{110x}	504.0	6.94	1685
E _{110y}	522.9	5.37	988
E _{120x}	950.5	18.9	4951
E _{120y}	958.7	15.2	4292

For our simple test cavity, finding eigenmodes was easy. In a realistic LIA accelerating module, this approach will be complicated by a large number of modes. The alternative method – well suited for cavities with low- Q resonances – is calculating impedances from wake potentials. We use a rigid longitudinal Gaussian charge distribution with the r.m.s. length 5 cm. Its frequency spectrum extends above 2 GHz and covers the frequency range of interest. The CST wake solver calculates up to 50 m of wake potentials left by the bunch as it propagates through the ferrite-loaded cavity along a path parallel to the beam axis but displaced by $d = 1$ cm either vertically or horizontally. Imposing proper boundary conditions at $x = 0$ and $y = 0$ allows using only one quarter of the cavity for calculations. The Fourier transform of the potential normalized by the bunch spectrum gives transverse wake impedances (measured in Ω). Divided by d , they give the transverse impedance Z_{tr} (in Ω/m). The transverse impedance for the test cavity with ring ferrite is compared with measurements in Fig. 3. There is only one resonance in the cavity, in agreement with Table 2; its calculated frequency agrees with the measured one but calculated peak value is 20% lower.

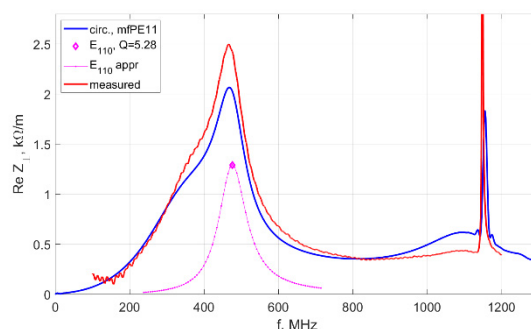


Figure 3: Transverse dipole impedance vs. frequency for the cavity with ring ferrite: calculated from wakes (blue), eigenmode contribution fit (magenta, cf. Table 2), and measured on test stand (red).

The sharp peak near the pipe H-mode cutoff frequency of 1186 MHz is observed both in simulations and measurements. This is an artefact due to the test stand setup; it is removed from some measurement data that follow.

For the cavity with ferrite arcs, the calculated transverse impedances are compared with measurements in Figs. 4 and 5.

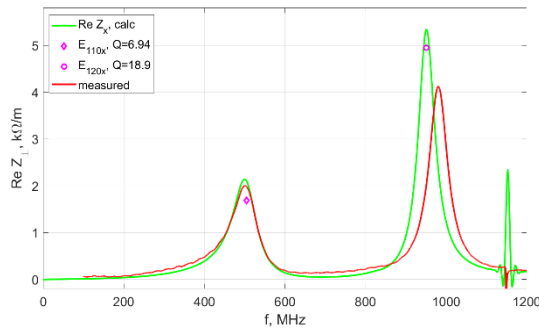


Figure 4: Horizontal dipole impedance vs. frequency for the cavity with ferrite arcs: from wakes (green), eigenmode peaks (magenta marks, cf. Table 3), and measured (red).

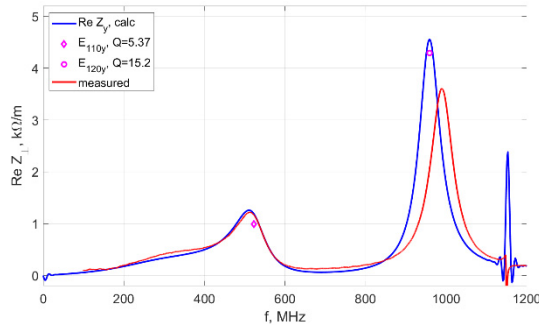


Figure 5: Vertical dipole impedance vs. frequency for the cavity with ferrite arcs: from wakes (blue), eigenmode peaks (magenta marks, cf. Table 3), and measured (red).

The calculated impedances agree well with the measured ones for the first resonance; even the shoulder below peak in Fig. 5 is resolved. For the second resonance, the calculated frequencies are somewhat lower while peak values are higher than measured ones.

For comparison, we plot in Fig. 6 the vertical transverse impedance calculated from wakes in the cavity with arcs of different ferrites, C2050 and CN20 [7], whose permeability is shown in Fig. 2. Similar to Fig. 5, calculations agree well with measurements for the first peak, but predict slightly lower frequencies and higher impedances for the second.

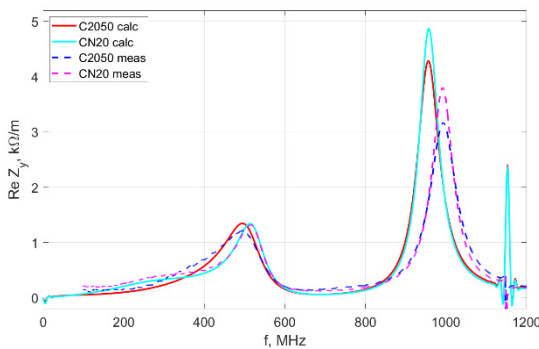


Figure 6: Vertical dipole impedance vs. frequency for the cavity with arcs made of different ferrites: calculated (red, cyan) and measured (blue, magenta – dashed).

Overall, there is a reasonable agreement between calculated and measured results. We attribute differences to the

influence of wires: even without ferrites the frequencies of dipole resonances measured by driving wires are shifted compared to those in Table 1. Better knowledge of ferrite properties will help improving calculation accuracy. Nevertheless, we can use the developed method of impedance calculation to evaluate different ferrite configurations in more realistic and complicated cavities.

As an example, we show in Fig. 7 the transverse impedance calculated and measured for a prototype Scorpius accelerator cavity. The outer part of the prototype cavity includes 8 induction cells and three sets of ferrite arcs near the gap region. This part of the cavity is separated from the beam pipe region by a plastic break in the gap and filled with oil. In the wake calculations for Fig. 7, a typical value for transformer oil permittivity, $\epsilon = 2.2$, was used.

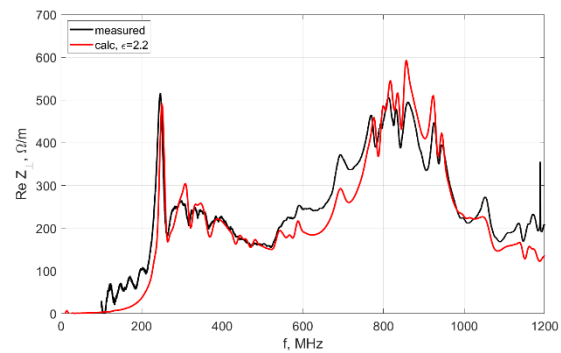


Figure 7: Transverse impedance vs. frequency for the prototype Scorpius cavity: calculated (red) and measured.

The agreement between calculations and measurements in Fig. 7 is good. We also performed mode calculations for this cavity with CST non-linear eigensolver to understand the field patterns and found 157 modes below 930 MHz. The peak near 240 MHz is produced by a single mode with $Q = 27.8$, while the wide peak at 800-900 MHz is caused by multiple overlapping modes.

CONCLUSION

We have developed an efficient method of calculating impedances in cavities with dispersive ferrites. A simple test cavity with or without ferrite inserts was studied as an example. The cavity transverse coupling impedances are also measured on a test stand using a two-wire method. The results of impedance calculations and measurements are in agreement. This method gives us a convenient tool to evaluate various design options and guide the design process.

The authors acknowledge and grateful for useful discussions with M. Crawford, G. Dale, and C. Ekdahl (LANL), and N. Pogue (LLNL).

REFERENCES

- [1] C. Ekdahl and R. McCrady, "Suppression of Beam Breakup in Linear Induction Accelerators by Stagger Tuning", *IEEE Trans. Plasma Sci.*, vol. 48, no. 10, pp. 3589-3599, Oct 2020. doi:10.1109/TPS.2020.3019999
- [2] L. Walling, M. Burns, D. Liska, D. E. McMurry, and A. H. Shapiro, "Transverse Impedance Measurements of Prototype Cavities for a Dual-Axis Radiographic Hydrotest (DARHT)

- Facility”, in *Proc. 14th Particle Accelerator Conf. (PAC'91)*, San Francisco, CA, USA, May 1991, pp. 2961-2964.
- [3] J. F. DeFord, G. D. Craig, and R. McLeod, “The AMOS (Azimuthal Mode Simulator) Code”, in *Proc. 13th Particle Accelerator Conf. (PAC'89)*, Chicago, IL, USA, Mar. 1989, pp. 1181-1184.
- [4] CST Studio Suite,
<https://www.3ds.com/products-services/simulia/products/cst-studio-suite>
- [5] M. Crawford and J. Barraza, “Scorpius: The development of a new multi-pulse radiographic system”, in *Proc. IEEE 21st Int. Conf. Pulsed Power*, Brighton, U.K., 2017, pp. 1–6.
- [6] J. DeFord *et al.*, “Development and application of dispersive soft ferrite models for time-domain simulation”, Livermore, CA, United States, Rep. UCRL-JC-109495, 1992.
- [7] National Magnetics Group, Inc.,
<https://www.magneticsgroup.com>
- [8] A. W. Chao *et al.*, *Handbook of Accelerator Physics and Engineering*, World Sci., 2013.